Hindawi
Mobile Information Systems
Volume 2022, Article ID 5850967, 12 pages
https://doi.org/10.1155/2022/5850967

Research Article

The Model of Ceramic Surface Image Based on 3D Printing Technology

Hui Yu,[1] Enze Chen,[2] Yao Chen,[2] and Zhenyu Qi[3]

[1]*Department of Arts, Nanchang University, Nanchang 330000, China*
[2]*Department of Ceramic Arts, College of Music and Arts, Dankook University, Yongin-si 16890, China*
[3]*Department of Art and Design, Hubei University of Technology, Wuhan 4300068, China*

Correspondence should be addressed to Enze Chen; sqqm@jou.edu.cn

Received 16 May 2022; Revised 20 June 2022; Accepted 23 June 2022; Published 30 July 2022

Academic Editor: Wen Zhou

With the rapid development of the new manufacturing industry, 3D printing technology continues to make new technological breakthroughs, and new works emerge in the manufacturing, medical, construction, military, and other application fields. However, for ceramic materials, there are still many problems to be solved in 3D printing. In this study, a dual-scale lightweight interactive model based on lofted surface and periodic parameter curve embedding is proposed for ceramic 3D printing. Users can model and manufacture lofted surfaces with small-scale geometric textures. For the two closed curves entered by the user, the intermediate section sampling points are generated by interpolation between them, and the shape of the current surface is adjusted under ceramic 3D printing manufacturing constraints such as no support and path non-interference. complete large-scale surface modeling based on lofted surfaces. Then the straight line path between the sampling points is replaced by a periodic curve path, and the small-scale geometric texture modeling is completed by adjusting the period and amplitude of the curve function. Finally, each section sampling point is spirally connected layer by layer and directly generats a single continuous printing path and manufacture. The experimental results show that the tool provides users with sufficient modeling space and high efficiency of model generation and effectively generates G-code files with textured lofted surfaces that can directly print ceramic 3D. It can also avoid the collision between printer nozzles and printing models and can be directly used in 3D printing and manufacturing based on clay materials.

1. Introduction

3D printing (also known as material added manufacturing) technology appeared in the mid-1990s. With the rapid development of various science and technology, 3D printing technology has also improved. In the fields of manufacturing, medical, construction, and military applications, new technological breakthroughs and new products have emerged [1]. Experts in many fields generally believe that 3D printing technology will profoundly change the future society and will be the development direction of manufacturing informatization and intelligence in the future. At the same time, some industrial product manufacturing enterprises and traditional handicraft workshops are gradually losing competitiveness and meeting the bottleneck of development due to the influence of industrial manufacturing and processing technology on product form [2]. Through the analysis of some innovative application cases of 3D printing technology at home and abroad, the author summarizes several development trends of product forms based on 3D printing technology in the future, combines the Internet business thinking and product customization trend, and concludes that some industrial manufacturing enterprises and handicraft workshops are in the bottleneck. The conclusion of customized products based on 3D printing technology should be actively developed, which can provide ideas and references for the development of enterprises.

Predecessors have done some work on the flow analysis of the single screw extrusion process, but most of them are realized by commercial numerical calculation software, such as fluent and POLYFLOW. In essence, such software realizes the calculation and analysis by solving the differential equations to

obtain the solution of the Navier Stokes equation. When solving the fluid with complex rheological characteristics, the calculation process is complex and easy to diverge. LBM is used to replace the traditional finite element method to analyze the flow of ceramic slurry in the screw groove, which ensures the stability of the numerical simulation process.

2. State of the Art

2.1. The Development of 3D Printing Technology. 3D printing technology is a rapid stereo-forming technology based on a digital model [3]. It is a technology that makes printing materials layer by layer and then forms solid shapes through data processing. Unlike the traditional manufacturing process for material reduction, 3D printing technology is formed by adding and forming layer by layer. This is also known as additive manufacturing. Since the first commercial 3D printer was published in the 1980s, 3D printing has been developing rapidly in the fields of printing materials, printing forming principle, and application [4].

Ceramic material is one of the three solid materials with excellent characteristics such as high hardness, high strength, high-temperature resistance, low density, good chemical stability, and corrosion resistance. 3D printing materials include photosensitive resin composite, polymer powder, paraffin powder, ceramic powder, fuse line, FDM ceramic, wood plastic composite, and FDM support material.

The principle of a 3D printer is similar to that of ordinary printers in daily life. However, ordinary printers use paper ink as raw materials in the two-dimensional plane to print. While the raw materials used by 3D printers are metal, plastic, ceramics, fibers, and other materials as printing materials. Through the calculation and analysis of digital models, the data is imported into 3D printers. The printer will stack the raw materials layer by layer according to the path completed by calculation, and finally form a three-dimensional solid shape after continuous stacking one layer by one.

printed by hot melt deposition technology is solidified by cooling, and the shape printed by liquid deposition technology is cured by drying. SLS is formed and solidified by laser heating, ultraviolet irradiation, adhesive bonding, etc. Under the control of data calculation, the laser beam fused the single layer of the powder with precise coordinates, and then sintered selectively to form the solid shape. The photo-curing molding (SLA) uses UV light to precisely irradiate the photosensitive resin to make the photosensitive resin solidify. It can be cured by moving vertically to the second layer for irradiation curing, and then forming a solid shape after the irradiation curing layer by layer. And the layer solid manufacturing (lom > uses a computer-controlled laser to cut the thin film, paper, and other sheet materials accurately and form the solid shape by layer bonding between each layer [6].

With the continuous development of science and technology, the application field of 3D printing technology is also expanding. It is not only the processing of simple parts but also has many applications in the fields of national defense science and technology, aerospace, medicine, housing construction, automobile, electronics, food, clothing, etc. In 2014, ten 3D printing buildings appeared in Shanghai. In 2016, the first space in orbit 3D printer was developed by the Chinese Academy of Sciences. In 2019, the spinal cord scaffold which imitated the structure of the central nervous system was successfully made by 3D printing technology [7].

2.1.1. It Can Be Applied in Many Fields. When using 3D printing services to process products, we can obtain very fast speed. Therefore, 3D printing technology has received great attention in all walks of life, which has promoted the rapid development of this technology and has been widely used in consumer electronics, automobiles, aerospace, medical treatment, military industry, geographic information, art design, and other fields. At the same time, 3D printing can also be combined with metal castings and extended to many industrial fields.

2.1.2. Be Able to Concretize Conscious Products. In terms of the development trend of academic ideas, 3D printing services have not been widely used. Technology is developing from the past shape manufacturing to the integration of material organization structure and shape structure design and manufacturing. R&D personnel are trying to realize controllable manufacturing from micro-organization to macrostructure, so they can make conscious products more specific so that people can quickly understand them.

2.1.3. Shorten the Development Cycle of New Products. The use of a 3D printing service can quickly turn the design drawings into real models, so as to intuitively analyze and understand the deficiencies in the design structure. Therefore, it plays a positive role in promoting product innovation and shortening the development cycle of new products.

When obtaining products through 3D printing services, there is no need to prepare any molds, cutting tools, or tooling fixtures. 3D printing equipment can directly accept product design data and quickly manufacture samples, molds, and prototypes of new products. Therefore, the 3D printing service not only has a wide range of application fields but also can greatly shorten the development cycle of new products.

2.2. The Historical Development of 3D Printing Technology. In 1883, chuck hill, an American scientist, invented the technology of photo-curing 3D printing.

In 1886 chuck Hill established a 3D systems company, and launched the first commercial 3D printer, which promoted 3D printing technology.

Scott Crum and Lisa Crum jointly invented the melt deposition forming technology (FDM) in 1888 and established STRATASYS company to promote related business.

In 1995, the United States took the lead in developing 3D printers [8].

In 2005, the first 3D printer, spectrum 2510, developed by the z-crop company in the United States, was successfully developed to print high-definition and multi-color shapes.

In 2011, the world's first 3D printing aircraft was successfully developed [9].

Scottish scientists used 3D printing technology to create the first human liver tissue in 2012.

In 2018, human beings first printed biological organs in space using biological 3D printing technology.

Since the early 1990s, the research on additive manufacturing technology has been launched with the support of government funds from Tsinghua University, Central China University of Science and Technology, and the Research Institute of West Jiaotong University. Shaanxi Hengtong Intelligent Machine Co., Ltd. (Xi'an Jiaotong University), Shanghai Liantai Technology Co., Ltd.: light curing rapid prototyping (SLA), Wuhan Binhu electromechanical Co., Ltd. (Huazhong University of Science and Technology), Beijing Longyuan automatic molding system Co., Ltd.: powder laser sintering rapid prototyping (SLS), Tsinghua University: melt deposition rapid prototyping (FDM), Northwest University of Technology Beijing University of Aeronautics and Astronautics: laser cladding equipment (lens) Huazhong University of science and technology, South China University of Technology, Nanjing University of Aeronautics and Astronautics: metal powder laser melting (SLM) after 2011, the number of enterprises engaged in SLA, SLM, FDM, DLP, lens, and other processes has increased year by year. At present, the domestic additive manufacturing system can meet the production needs of conventional materials and processes. In 2019, the national output value of 3D printing was 10 billion yuan, and in the first three quarters of 2020, the national output value was 10 billion yuan. In 2019, Aikang medical and platinum were listed; In 2020, Maipu medical will be listed. In general, compared with the development history of foreign companies for more than 30 years, domestic 3D printing equipment started late. Although rapid progress has been made in a short time, it needs to be further improved in terms of equipment operation stability and product quality. It is still a distance from the goal of domestic substitution for import and agency to self-sale. However, with the continuous expansion of downstream application fields, domestic manufacturers are expected to achieve breakthroughs in subdivided fields.

2.3. 3D Printing Technology for Ceramic Product Forming. As a new rapid prototyping technology, 3D printing technology constructs the digital model in space in the direction of layer-by-layer printing. With the rapid development of 3D printing technology, there are also a lot of printable materials. The common materials are resin, metal, rubber, cement, paper, ceramics, etc., as chemically stable materials that have been used in 3D printing for a long time. Unlike the traditional ceramic manufacturing process, the traditional ceramic products are mostly formed by the relationship between humans and mud. This way often needs to have. 3D ceramic printing is designed by using a computer model scheme, and then the model is processed by slicing software, which becomes a kind of data that can be recognized by the printer, and finally imported into the printer for printing and presentation. Such a series of treatments change the relationship between man and mud into the relationship between man and number. Now, 3D printing technology can be used in ceramic molding, mainly including 3D printing of liquid deposition ceramic and ceramic powder printing. Indirect molding is to select the 3D printing technology of photosensitive resin, 3D printing technology of hot melt plastic, printing technology of paper material, etc., to turn the gypsum mold and then use the mold to assist in the molding of ceramic [10].

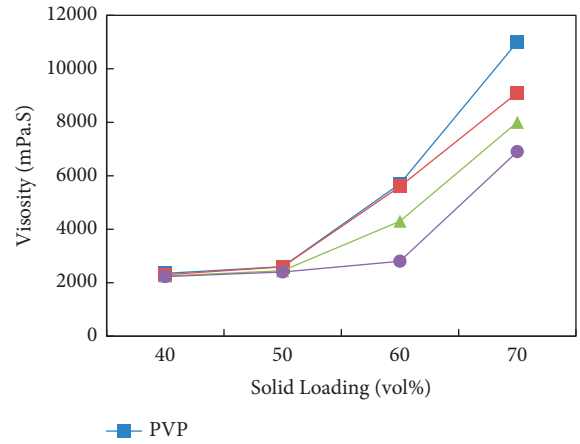

Figure 1: Viscosity of ceramics with different dispersants.

With the development of 3D printing technology and its wide application in various fields, 3D printing for ceramic materials has attracted more and more researchers' attention. Ceramics have low density, high-temperature resistance and corrosion resistance, high mechanical strength and hardness, and good chemical stability. It is suitable for aerospace, biomedical, chemical, electronic, and mechanical fields. Compared with traditional ceramic manufacturing technology, 3D printing-based ceramic manufacturing efficiency is high and the process is simple, especially in the generation of complex geometric structures or high precision models. Many materials can be used in the 3D printing of ceramics, such as concrete, engineering ceramics, and bioceramics. However, clay materials are widely used in buildings and infrastructure. Figure 1 shows the ceramic viscosity under different dispersant conditions. When different dispersants are used and the proportions of dispersants are different, ceramic materials can exhibit significantly different viscosities. This expands the application scope and field of clay materials to a certain extent.

Figures 2 and 3 show the effects of milling time and dispersant content on the viscosity of the ceramic slurry, respectively. Analysis of these performance maps shows that the ceramic materials required for 3D printing are not only easy to obtain but also can obtain different properties under different conditions, which is a good 3D printing material. The effect of ball milling time on the viscosity of the ceramic slurry is given in Figure 2. With the increase in time, the components of the ceramic slurry are more dispersed and the viscosity decreases with time. When a certain time threshold is reached, the viscosity increases due to the repolymerization of the slurry components.

Ceramic clay materials are cheap and easy to obtain. Nowadays, the desktop-level 3D printer is becoming more and more popular. Users can easily take materials from the

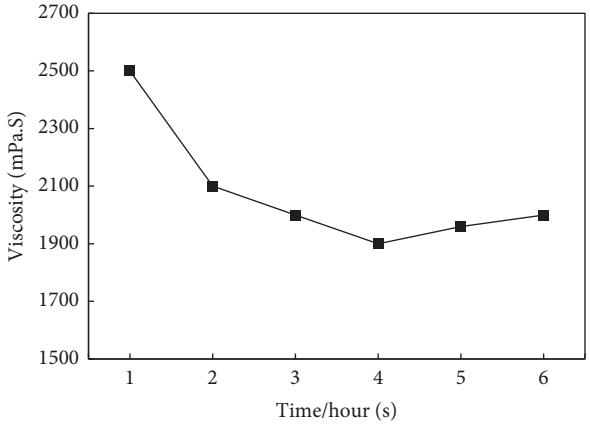

Figure 2: The effect of ball milling time on the viscosity of ceramic materials.

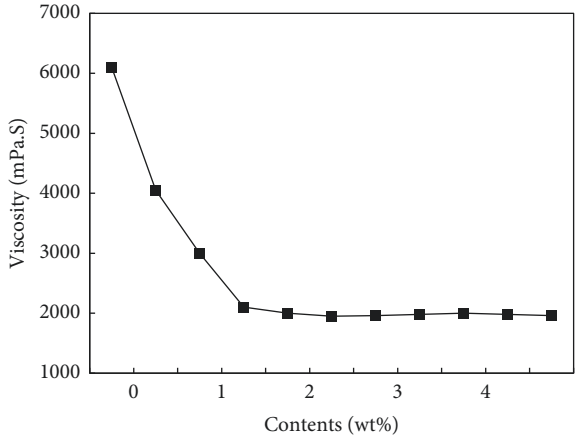

Figure 3: Effect of dispersant content on the viscosity of ceramic materials.

local area and make their own ceramic models to meet the needs of individuals. As a green and reusable printing material, unlike the thermoplastic materials used in general 3D printing processes, such as fused deposition modeling (FDM), ceramic clay materials will remain relatively soft throughout the printing process, and will not solidify rapidly after deposition [11]. If there is a free space for the moving nozzle between different printing areas, the formed part and nozzle will be deformed or damaged due to the adhesion of clay. Therefore, the design of ceramic material printing path requires that the model must be completed by a single continuous printing path. Because the removal of ceramic 3D printing support structure will cause some damage to the surface of the model, so the optimization of the model to the structure without support printing can improve the printing quality. In this study, the extrusion 3D printing technology based on ceramic material is adopted. When the height difference of the same layer in the z-axis direction exceeds the length of the printer nozzle, the printer nozzle will collide with the model being printed, which will cause the model to fail to print. Therefore, the corresponding printing constraints should be considered in modeling to avoid this situation. The rapid development of 3D printing technology makes it possible for users to customize their models. However, users usually need to create models with the help of professional CAD modeling software, and then generate paths based on existing slicing software. Modeling is very complex for ordinary users, and it can not guarantee the model without the support and no interference in the printing process, and can not meet the single continuity of generating print path. Based on Lofting technology and periodic parameter curve embedding, this study proposes a two-scale interactive modeling and manufacturing method for 3D printing of ceramics. In the modeling process, the model is supported and the printing process is automatically corrected without reconstruction of the discrete grid expression of the model [12]. After the model type is confirmed, a single continuous printing path is generated and the G-code file directly used for printing is output. The double-scale modeling proposed in this study (see Figure 4) is to generate lofting surface by user input control curve to realize large-scale geometry, and realize small-scale geometric texture based on periodic parameter curve. Manufacturing constraints are guaranteed by an automatic local correction in interactive design lofting surface. The experimental results show that the interactive modeling and manufacturing tool proposed in this study has simple operation and high G-code file generation efficiency; Compared with the existing slicing software, the tool supports model support free printing, meets the unique printing path, single continuity, and collision-free constraints of ceramic 3D printing, and improves the printing quality of physical model [13].

3. Methodology

3.1. Application of LBM in Herschel Bulkley Fluid. The raw materials for preparing ceramic slurry include pentaerythritol triacrylate and benzene couple as organic solvents. After mixing, lead lanthanum zirconate titanate powder (PLZT) is evenly added. At the same time, high-speed stirring helps the powder dissolve rapidly, and finally, a standby slurry with a solid content of 68.6% is obtained. After the slurry is prepared, its viscosity needs to be tested to obtain its rheological equation to prepare for subsequent numerical simulation analysis. Here, it is planned to use a rotary viscometer (model: rheolab MC1) to measure the viscosity of the mixed fluid. The results show that the slurry shows obvious non-Newtonian characteristics of shear thinning. According to the fitting results of MATLAB software, the rheological equation of the slurry tends to the type of Herschel Bulkley fluid.

The schematic diagram of the 3D printing ceramic forming process is shown in Figure 5. The alumina ceramic slurry is printed and formed by ceramic 3D printing technology. After that, the light-cured alumina ceramic slurry with the optimal dispersant and alumina slurry powder was printed layer by layer by a self-developed DLP type ceramic 3D printer.

LBM describes the motion process of fluid particles by solving the equation of equilibrium, which is a specific evolution equation

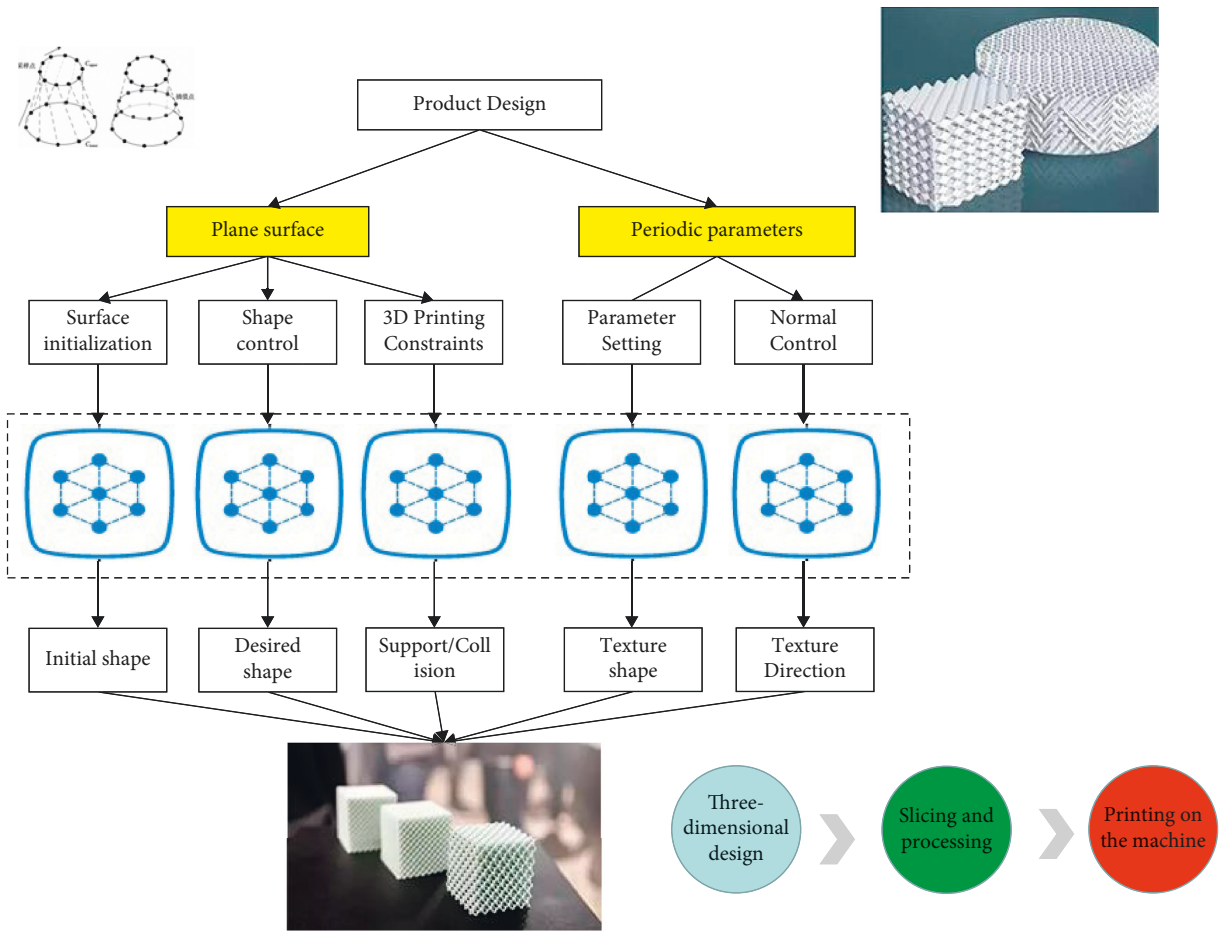

Figure 4: 3D ceramic printing scheme designed in this study.

$$f_i(r + e_i\delta t, t + \delta t) = -\frac{1}{\tau}[f_i(r,t) - f_i^{eq}(r,t)], \tag{1}$$

where τ-The relaxation time and velocity vector EI can be obtained by:

$$\begin{cases} (0,0), & i = 0, \\ c\left(\cos\dfrac{i-1}{2}\pi,\ \sin\dfrac{i-1}{2}\pi\right), & i = 1,2,3,4, \\ \sqrt{2}\,c\left(\cos\dfrac{2i-9}{4}\pi,\ \sin\dfrac{2i-9}{4}\pi\right), & i = 5,6,7,8. \end{cases} \tag{2}$$

The lattice speed c depends on the step size of the grid δX and time step δt. The specific relationship is $C = \delta x/\delta t$。. Generally, both are taken as 1, and C is also 1. The equilibrium equation is mainly affected by density ρ. The specific relationship between the influence of velocity u is as follows:

$$f_i^{eq} = \omega_i\rho\left[1 + \frac{e_i \cdot u}{c_s^2} + \frac{(e_i \cdot u)^2}{2c_s^4} - \frac{u^2}{2c_s^2}\right]. \tag{3}$$

According to the formula, we can see that due to the influence of the fluid equilibrium state, when the density of the fluid is greater, the speed of the fluid motion is slower; when the speed is greater, the density of the fluid will decrease. For the D2Q9 model, the sound velocity CS = $c/3$, and weight parameter ω, the specific form of I is shown in the formula

$$\omega_i = \begin{cases} \dfrac{4}{9}, & i = 0, \\ \dfrac{1}{9}, & i = 1,2,3,4, \\ \dfrac{1}{36}, & i = 5,6,7,8. \end{cases} \tag{4}$$

According to the distribution function, the macro expressions of velocity, density, and pressure are, respectively,

$$\begin{aligned} \rho &= \sum_i f_i^{eq}, \\ \rho u &= \sum_i e_i f_i^{eq}, \\ P &= \rho c_s^2. \end{aligned} \tag{5}$$

According to the isotropic constraints, we can get the following:

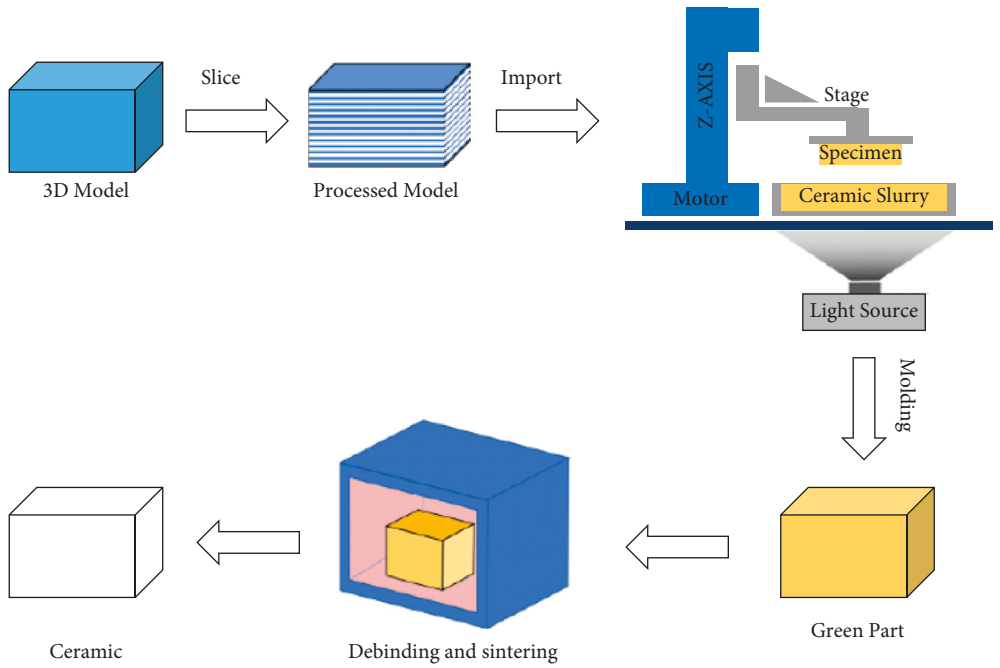

Figure 5: Schematic diagram of the process of 3D printing ceramic molding.

$$\sum_i f_i^{eq} e_{ix} e_{iy} = \rho u_x u_y + P\delta_{xy} = \rho u_x u_y + \frac{1}{3}\rho\delta_{xy}, \tag{6}$$

where δXY is the croceck function. Based on Chapman Enskog, the distribution function and momentum tensor can be extended to:

$$f_i \approx f_i^{eq} + \varepsilon f_i^{(1)} + \varepsilon^2 f_i^{(2)}, \quad \prod_{xy} \approx \prod_{xy}^{(0)} + \prod_{xy}^{(1)}. \tag{7}$$

By solving the primary moment of velocity, the momentum tensor of equilibrium state π XY (0) and the momentum tensor of non-equilibrium state π XY are solved.

(1) It can be calculated by the following formula

$$\prod_{xy}^{(0)} \sum_i e_{ix} e_{iy} f_i^{eq} = P\delta_{xy} + \rho u_x u_y, \prod_{xy}^{(1)} \sum_i e_{ix} e_{iy} \left(1 - \frac{1}{2\tau}\right) f_i^{(1)}. \tag{8}$$

For non-Newtonian fluids such as Herschel Bulkley fluid, the formula for the strain rate tensor s_{xy} is as follows:

$$S_{xy} = -\frac{1}{2\rho\tau e_s^2} \sum_i e_{ix} e_{iy} f_i^{(1)}. \tag{9}$$

The relationship between dynamic viscosity relaxation time τ and density ρ is:

$$\mu = \rho\nu = \frac{(2\tau - 1)\rho}{6}. \tag{10}$$

3.2. Flow Simulation in the Extrusion Process of Slurry Direct Writing. Path planning is a basic problem in 3D printing. At present, there has been a lot of work on this problem. The commonly used path planning algorithms include zig-zag scanning algorithm, contour parallel line algorithm, space-filling curve algorithm, and so on. Due to the angle between the model surface and the printing direction in the process of 3D printing, the zig-zag scanning algorithm is easy to produce underfill or overfill errors, which will affect the printing accuracy. The contour parallel line algorithm avoids the problem of printing accuracy by calculating a series of equidistant lines parallel to the contour. However, when the shape is complex, there will be too many empty strokes between parallel contour lines. The space-filling curve has attracted more attention because of its continuity, such as the continuous Fermat curve filling algorithm.

The two-scale modeling tool proposed in this study carries out large-scale parametric design through lofting and obtains the basic geometry of the object It can reduce the amount of surface data and ensure the continuity of the surface.

Take section Y-Z as the analysis surface. According to the actual rotation, it can be seen that the speed should only be set on the upper surface and the speed direction is parallel to the Z axis. The speed in the remaining three directions is set to 0. According to Table 1, the width and depth of the screw groove are all 4 mm, and the lattice number is 120 in numerical simulation × 120, the speed of screw $n = 45$ r/min. As

Table 1: Formulation of photosensitive resin paste.

Reagent	PEG	ACMO	PPTTA	TPO	HQ	Findan orange G	BYK
Mass fraction	30	28	37.99	1	1	0.01	2

LBM is a dimensionless method, dimension conversion is needed when the actual simulation analysis is carried out. Here, Reynolds number Re is used as the criterion number, and then the conversion process can be realized by combining similar criteria. The streamlined diagram can be obtained by numerical analysis. The upper side of the cross-section flow area is the inner wall of the outer cylinder of the screw, and the left and right sides are respectively two wall surfaces of the screw groove, and the lower side corresponds to the outer wall of the screw rod core. The center of the flow field is near (2 mm, 2.7 mm). From the position, it is closer to the inner wall of the outer cylinder of the screw rod, and there is bidirectional flow in the depth direction of the screw groove. The whole flow is carried out in circulation. There is no obvious flow in the lower left and right corners. In the later optimization of the structure, the angle between the screw edge and the rod core can be increased rather than the current vertical welding.

The distribution of velocity component V in different directions is given respectively. The comparison is made when the depth of different screw grooves and width of the slot is taken. Combining the two figures, it can be found that the velocity component V is basically 0 in the middle of the channel. As it approaches the edge of the screw, the speed changes gradually. Due to the different depth of the spiral groove, the velocity component V is also significantly different. The maximum value of V appears in the center of the flow field and is smaller when it is close to the boundary.

The distribution of velocity component u in different directions is given, respectively. The comparison is made between the different depths of the screw groove and the width of the slot. Combining the two graphs, it can be found that the velocity component u is close to 0 near the wall of the screw edge. When the velocity is gradually away, the velocity changes gradually, and the corresponding velocity is different with different groove depths, The closer the inner wall of the outer cylinder of the screw, the greater the velocity component U.

The concept of slurry direct writing molding technology was first proposed by Cesarano et al. This technology carries out the pre-design of graphics through computer-aided manufacturing, and the computer controls the movement of the slurry conveying device installed on the z-axis on the X-Y platform to obtain the required graphics. After the first layer is formed, the z-axis rises to an appropriate height, and the structure of the first layer is formed on the basis of the first layer. Through repeated superposition and the addition of materials, a fine three-dimensional structure is finally obtained. Slurry direct writing technology appeared earlier and began to be called robocasting. It was not included in the category of 3D printing until recent years. Therefore, it is called a new 3D printing technology.

In the traditional slurry direct writing process, the extrusion part adopts the needle barrel structure, which realizes the extrusion movement in the form of pump pressure. In addition to this extrusion method, screw extrusion, as an effective transportation extrusion method, is widely used in food processing, polymer materials, and mechanical fields. It is proposed to use screw extrusion to replace the common needle barrel structure.

As an effective transportation extrusion method, screw extrusion is widely used in food processing, polymer materials, and mechanical fields. Domain screw extrusion is plastic. It carries out solid transportation, compaction, melting, shear mixing, and extrusion of a plastic through external power transmission and heat transfer of external heating elements. The needle cylinder structure realizes extrusion movement in the form of pump pressure.

Aiming at the 3D printing technology of slurry direct writing ceramic, a screw structure instead of a needle barrel extrusion structure is proposed [14]. The formula of photosensitive resin paste is shown in Table 1. LBM is used to replace the traditional finite element method. The flow of ceramic slurry in the screw groove is analyzed, which ensures the stability of the numerical simulation process. The following conclusions can be obtained: (1) It is found by viscosity test and the ceramic slurry involved belongs to a typical shear thinning non-Newtonian fluid. (2) Through the rational application of LBM, the numerical solution is successfully obtained, which further widens the effective application of LB in the field of engineering application; (3) According to the obtained figure, the flow of ceramic slurry in the cross-section presents the characteristics of circulation, and the streamline diagram can be used to judge the effective flow area of ceramic slurry in the screw groove, and there is no obvious flow in the left and right lower corners of the cross-section; (4) In order to enhance the flow of ceramic slurry, the rotating speed can be appropriately increased and the groove width of the screw can be widened [15].

After mapping the two closed contour curves Cupper and Clower entered by the user to the $z = H$ plane and $z = 0$ plane in the world coordinate system, calculate the leftmost and rightmost endpoints of the two curves in the x-axis direction, respectively, and align Cupper and Clower based on the midpoint of the endpoint line. Please note that this tool not only supports users to draw contours directly based on spline curves but also supports users to load images with curves. The system will automatically extract continuous pixels in the image and generate contour curves. The large-scale modeling process of this study is as follows: based on the lofting technology, the interpolation operation is carried out between Cupper and Clower to generate multiple intermediate sections [16], and then the control line is used to adjust the current surface shape. For the model with support, because removing the support after printing will damage the

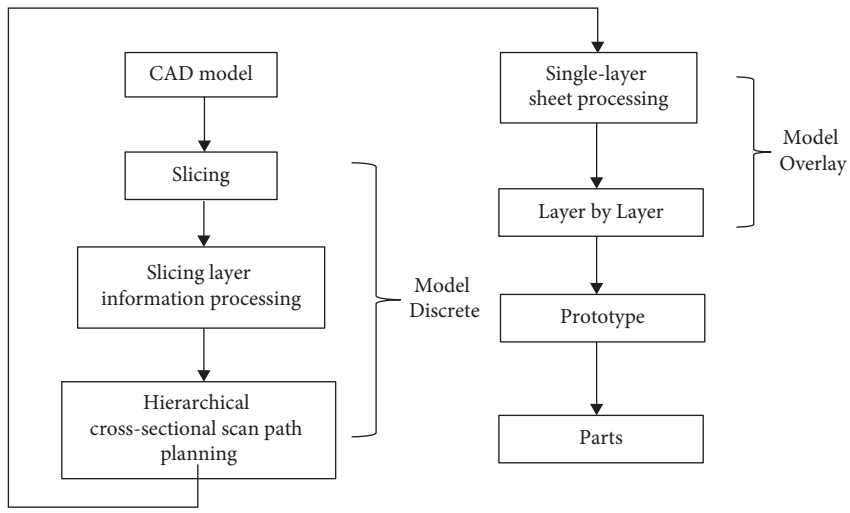

Figure 6: 3D printing workflow.

Table 2: Printing parameters.

Brightness	Delaminating thickness	Exposure inch same (s)	Base layer monolayer exposure time (s)	Light intensity
65	25 um	2	15	20

surface of the model, in order to ensure support-free printing, it is necessary to correct the model without support to ensure that the model will not have an area with too large inclination. At the same time, in order to avoid the collision between the printer nozzle and the printing model, the height difference between the highest point and the lowest point of the model on the same printing layer shall not exceed the length of the printer nozzle. See Table 2 for printing parameters. (Algorithm 1)

3.3. Ceramic 3D Printing Manufacturing Constraints. First, the suspension structure of the part is identified and segmented; then the three-dimensional model of the suspension structure is transformed by spatial rotation; afterward, the rotating structure is sliced; and then the slicing code is rotated reversely to the original position. Finally the transformed code is coupled. This method has the advantages of low algorithm complexity, high integration, and strong expansibility. It has universal applicability in the fields of biological 3D printing, light curing 3D printing, and so on.

In this study, an extruded ceramic 3D printer based on clay is used. In view of the particularity of clay materials, three manufacturing constraints are mainly considered in the modeling process (1) Support free constraint in the ceramic 3D printing process. For the part of the model whose inclination is greater than the threshold, if the support structure is not added, it is easy to collapse in the printing process [17]. Therefore, this study proposes a support-free algorithm, which realizes support-free printing by locally adjusting the inclination of the model, avoids the damage to the model surface caused by removing the support, and improves the printing quality of the model. (2) Collision-free constraint between printer nozzle and model. Ceramic 3D printing requires that the maximum height difference of each layer of the printing path in the z-axis direction should not exceed the length of the printer nozzle, otherwise there will be a collision between the printing model and the printer nozzle, resulting in printing failure. In this study, the height difference threshold is set in the horizontal control line adjustment to ensure that the height difference of each layer in the printing path is not greater than the length of the printer nozzle [18]. (3) Single continuous print path constraint. Clay is a fluid material with strong viscosity. When there is an empty stroke of moving the nozzle in the process of model printing, the strong adhesion between the newly extruded clay and the previously printed model will lead to model deformation and even printing failure [19].

We carried out the inclination test experiment, with inclination angles of 45°, 50°, and 55°, respectively. It can be seen that when the layer thickness is 0.25 mm, the physical quality of the printed models under the three dip angles is good. After measurement, the error between the actual physical dip angles of the three models and the original digital model is small and can be ignored. However, when the layer thickness is 1.0 mm, the upper half of the model has obvious outward convex deformation under the inclination of 50°, while the upper half of the model collapses under the inclination of 55°, and the actual physical model under the inclination of 45° is similar to the original digital model. To sum up, 45° inclination can ensure the reliable printing of the model, so this study takes 45° as the maximum safety angle threshold of the model relative to the vertical direction, as shown in Table 3.

3.4. Small Scale Modeling Based on Periodic Parameter Curve. Lofting surface generation based on large-scale modeling can only control the shape of the model microscopically, and

Input: Upper top surface contour curve cupper, lower bottom surface contour curve Clower, model height H
Output: G-code file that can be used for 3D printing of ceramics.
Step 1. Make equidistant sampling on Cupper and Clower to generate the same number of sampling point sets Cupper and Clower, and establish one-to-one correspondence based on the drawing order
Step 2. Linear interpolation is made between Cupper and Clower to generate sampling points in the middle section
Step 3. Under the constraint of ceramic 3D printing manufacturing, adjust the control line and recalculate the coordinates of sampling points on the current surface
Step 4. Select the periodic curve to be embedded into the horizontal and vertical directions in the current parameter space, and adjust the curve period and amplitude to generate geometric texture
Step 5. The sampling points on each section are connected layer by layer in a spiral way to generate a printing path
Step 6. Generate G-code files that can be used for 3D printing of ceramics (see Figure 6).

Algorithm 1: Two-scale lofting surface modeling algorithm.

Table 3: Analysis and comparison of advantages and disadvantages of 3D printing materials.

Material name	Advantages	Shortcomings
ABS PLASTICS	(1) It has excellent mechanical properties and excellent pullout strength	(1) Printing a large area of products is easy to raise
	(2) Easier to remove support	(2) The platform needs to be heated to $80^{\circ}C \leq 120^{\circ}C$
PLA PLASTIC	(1) Biodegradable materials, environmental protection (2) The printing product has a high gloss (3) Good liquidity, printing is not easy to crack (4) It is not easy to print a large area of products (5) The printing process has no odor	(1) It is not easy to remove support (2) The impact resistance is relatively low

can not generate a model with rich geometric details. Therefore, this study controls the shape of the model by embedding various periodic parameter curves in the current surface parameter space. In this study, the directions of any two corresponding points in Cupper and Clower and the interpolation points between them are abstracted as y direction, and the directions of points located in the same section layer are abstracted as X direction. Select the periodic parameter curve in the X direction and Y direction respectively for embedding, that is, the connecting line between two points in these two directions is replaced by the periodic parameter curve. From left to right, the three models are embedding triangular wave curve in X direction, embedding triangular wave curve in Y direction, and embedding triangular wave curve in two directions at the same time, and multiplying the function values of the two directions. By adjusting the period of the periodic parameter curve (the number of sampling points in a period) and the amplitude of the curve, rich and detailed geometric textures can be generated on the surface of the model in this study, the amplitude direction is the normal direction of the surface [20].

For models with rich geometric details, the geometric texture is usually used for modeling. Bhat et al. proposed a sample-based geometric texture synthesis method, established the corresponding relationship between the sample model and the target model through training, and migrated the sample geometric texture to the target model according to the direction field given by the user.

Without considering small-scale modeling, embedding periodic curves directly on Cupper and Clower, and generating base note based on lofting, then adjusting the vertical direction control line to further adjust the shape of the model, the generated model can also present a certain scale geometric texture feature. The cupper and follower of the model are petal curves with the shape of the lower left corner. However, the texture generation based on this method depends on the manual adjustment of control lines, the more fine the texture adjustment is, the more complex the texture adjustment is, and the consistency of curve period and amplitude cannot be guaranteed. The periodic curves embedded in the top and bottom surfaces are the same as those. After large-scale modeling, triangle wave functions with periods of 10 and 2 and amplitude of 2 are embedded in the transverse and vertical directions respectively. It is obvious that the resulting geometric texture is more abundant and detailed than the large-scale modeling based on the sample placement.

In this study, three periodic curves, sinusoidal function wave, triangle wave, and square wave are provided for the user to choose. In this study, the sampling points on the contour line of the periodic curve to be inserted are discretely expressed as the value of independent variables.

A periodic function is a function whose value can be repeated after a certain period on any independent variable. For the function $y = f(x)$, if there is a constant t that is not zero, so that $f(x + T) = f(x)$ is true when x takes every value in the definition field, then the function $y = f(x)$ is called a periodic function, and the constant t that is not zero is called the period of the function.

Table 4: Data of different model.

Model name	Area (cm^2)	Mass (g)	Specific surface area (cm^2/g)	Results of the program
Lattice structure	332.72	10.32	32.24	Better
Cellular structure	312.33	19.68	15.87	General

Table 5: Formulation of ceramic slurry.

Material	Content (wt. %)	Content (vol. %)
Si_1N_4 powder	56.0	30.2
Yttium-aluminium-ganmen owder	6.2	2.3
Distilled water	24.9	42.8
Ethylene glycol	4.4	6.8
Dispersant (polyacrylic and carboxylic acid)	0.2	0.3
Ethanol	7.2	15.7
Lmsorganic binder	0.7	1.1
Deflocculant	0.4	0.8

Table 6: 3D printing method classification and comparison.

3D Printing technique	Strategy	Relative cost	Production time	Advantages	Disadvantages
Extrusion	Ceramic paste with polymer binder and plasticizer	Low—moderate	Slow	Straightforward process. Flexible in porous scaffolds or dense structures	Limited resolution
Binder jetting	Ceramic powder bed and polymer binder	Moderate -high	Moderate/ fast	Great for larger, porous ceramic structures. Requires few sacrificial materials	Challenging for very dense ceramics
Material jetting	Ceramic-suspended droplets on substrate	Low—moderate	Slow/ moderate	Beneficial for small models. Creates smooth surfaces	Difficult for large models
	Ceramic powder bed with laser	High	Fast	Flexible in porous scaffolds or dense structures	Distortion and warping leading to microcracks
Vat photopolymerization	Ceramic dispersed in photosensitive resin	Moderate	Moderate/ fast	Precise. Creates smooth surfaces	Requires extensive post-processing

$$f(t) = A\sin\left(\frac{2\pi t}{T}\right)$$
$$f(t) = A\left(\frac{4}{T}\left(t - \frac{2}{T}\left[\frac{2t}{T} + \frac{1}{2}\right]\right)(-1)^{[2t/T+1/2]}\right) \quad (11)$$
$$f(t) = A\text{sign}\left(\sin\left(\frac{2\pi t}{T}\right)\right).$$

4. Result Analysis and Discussion

Rapid and effective data processing can effectively improve the accuracy and strength of formed parts and the manufacturing efficiency of the equipment. (1) The analysis and processing technology of STL files in ASCII plain code and binary format, and the realization of core functions by Java programming language; (2) Based on STL file visualization, the topological relationship of common edges between two triangular patches, the support algorithm based on the topological relationship of triangular patch coordinate points and triangular patch meshing, and the advantages of feature region method and discrete identification method are combined to realize the generation of the support structure of STL 3D model from any perspective, And the time of support generation is greatly shortened, as shown in Table 4.

The algorithm is implemented by c++. The operating environment is 4 core intel core i5 CPU, 2.5 GHz main frequency, and 8 GB memory. Using the ceramic 3D printer cerambot plus print model, the printer has a shaping size of 180 mm (width) × 190 mm (deep). The minimum thickness is 0.25 mm, the maximum layer thickness is 1.0 mm, and the line width is 3.0 mm. The length of the nozzle of the ceramic 3D printer used in this experiment is 30.0 mm. The 3D printing technology of ceramic is based on the direct writing technology of fluid slurry. The technology makes the model at room temperature. This tool provides the user with an interactive interface, which can directly set the actual physical height of the model and the actual physical size corresponding to the current canvas edge length. In the process of 3D printing file generation, the sampling points and interpolation points on the top, bottom, and middle section layer are taken as the moving positions of printer nozzles; Then calculate the moving speed and extrusion amount of the printer nozzle at each position, and connect all points in spiral way layer by layer to generate the final

printing path and model G-code file, and the corresponding physical printing results. In this study, the method of Zhong and others is used in calculating the extrusion amount of clay. In order to ensure the single continuity of the printing path, for the model with a height difference in Z direction, this study calculates and adjusts the extrusion amount of ceramsite in real-time according to the distance change of Z direction of the sampling point, realizes the printing path with variable layer thickness, ensures the consistency of material volume per unit height of the path, and eliminates the step effect on the surface of the model Chen et al. In modeling and printing thin-walled shell, in order to minimize the step effect in the printing process, a modeling printing method combining multi-axis 3D printing technology and variable thickness surface slice technology is proposed. The work also generates a printing path with variable layer thickness, but it needs to be realized by multi-axis 3D printing technology. In this study, three groups of curves are drawn for the experiment. The results of sintering are printed according to the model. For the model generated by large-scale modeling based on lofting and the model with the texture generated based on the small-scale modeling, the printing time of the latter is 10–20 s longer than that of the former. Tables 5 and 6 analyze and compare the advantages and disadvantages of 3D printing materials to facilitate the selection of printing materials. The model and other models with texture are consistent in size and sampling point number.

5. Conclusion

In this study, a two-scale user interactive modeling and manufacturing tool based on Lofting surface is proposed for 3D printing of ceramics. The user can model and manufacture lofting surfaces with small-scale geometric textures. The print file can ensure a single continuous and unsupported print path, and avoid the collision between the printer nozzle and the print model. The experimental results show that the tool has high freedom and high efficiency, and the generated print file can be directly used in the ceramic model manufacturing of a 3D printer based on ceramic clay.

However, the method does not consider the influence of gravity in the modeling process. When the amplitude of the periodic function is too large, the drooping of the print path and even the collapse of the model may occur, which results in the difference between the physical model actually printed and the digital model presented in modeling. In addition, because the model with inclination exceeding the threshold can be optimized without support, it is impossible to model and manufacture the model with a larger inclination angle, and also can not model and manufacture the model with the height difference in Z direction greater than the length of printer nozzle. Finally, the volume of the ceramic 3D printing clay model will shrink by 10%–20% after sintering at high temperature. Hence, it can be explored in the future if the actual physical manufacturing results of the model can be predicted and the compensation optimization can be carried out in the future.

Data Availability

The labeled data set used to support the findings of this study is available from the corresponding author upon request.

Conflicts of Interest

The authors declare that there are no conflicts of interest.

Acknowledgments

This work was supported by Nanchang University, Dankook University, and Hubei University of Technology.

References

[1] Z. Chen, Z. Li, J. Li et al., "3D printing of ceramics: a review," *Journal of the European Ceramic Society*, vol. 39, no. 4, pp. 661–687, 2019.

[2] M. Schwentenwein and J. Homa, "Additive manufacturing of dense alumina ceramics," *International Journal of Applied Ceramic Technology*, vol. 12, no. 1, pp. 1–7, 2015.

[3] C. F. Revelo and H. A. Colorado, "3D printing of kaolinite clay ceramics using the Direct Ink Writing (DIW) technique," *Ceramics International*, vol. 44, no. 5, pp. 5673–5682, 2018.

[4] S. C. Park and B. K. Choi, "Tool-path planning for direction-parallel area milling," *Computer-Aided Design*, vol. 32, no. 1, pp. 17–25, 2000.

[5] Y. Yang, H. T. Loh, J. Y. H. Fuh, and Y G. Wang, "Equidistant path generation for improving scanning efficiency in layered manufacturing," *Rapid Prototyping Journal*, vol. 8, no. 1, pp. 30–37, 2002.

[6] X. Zhai and F. Chen, "3D printing path planning of fractal models," *Journal of Computer-Aided Design & Computer Graphics*, vol. 30, no. 6, p. 1123, 2018 (in Chinese).

[7] H. Zhao, F. Gu, Q. X. Huang et al., "Connected Fermat spirals for layered fabrication," *ACM Transactions on Graphics*, vol. 35, no. 4, pp. 1–10, 2016.

[8] J. Hergel, K. Hinz, S. Lefebvre, and B. Thomaszewski, "Extrusion-based ceramics printing with strictly-continuous deposition," *ACM Transactions on Graphics*, vol. 38, no. 6, pp. 1–11, 2019.

[9] F. Zhong, W. Liu, Y. Zhou, X. Yan, Y. Wan, and L. Lu, "Ceramic 3D printed sweeping surfaces," *Computers & Graphics*, vol. 90, pp. 108–115, 2020.

[10] S. Schaefer, J. Warren, and D. Zorin, "Lofting Curve Networks Using Subdivision surfaces[C]," in *Proceedings of the Eurographics/ACM SIGGRAPH Symposium on Geometry Processing*, pp. 103–114, ACM Press, New York, USA, July 2004.

[11] N. Engleitner and B. Jüttler, "Lofting with patchwork B-splines," *Advanced Methods for Geometric Modeling and Numerical Simulation*, Springer, Nora Engleitner, Bert Jüttler, pp. 77–98, 2019.

[12] N. Engleitner and B. Jüttler, "Patchwork B-spline refinement," *Computer-Aided Design*, vol. 90, pp. 168–179, 2017.

[13] A. Usumezbas, R. Fabbri, and B. B. Kimia, "The surfacing of multiview 3D drawings via lofting and occlusion reasoning [C]," in *Proceedings of the IEEE Conference on Computer Vision and Pattern Recognition*, pp. 4560–4569, IEEE Computer Society Press, Honolulu, HI, USA, July 2017.

[14] C. Y. Deng, J. Huang, and Y. L. Yang, "Interactive modeling of lofted shapes from a single image," *Computational Visual Media*, vol. 6, no. 3, pp. 279–289, 2020.

[15] P. Bhat, S. Ingram, and G. Turk, "Geometric texture synthesis by example[C]," in *Proceedings of the Eurographics/ACM SIGGRAPH Symposium on Geometry Processing*, pp. 41–44, ACM Press, New York, USA, July 2004.

[16] J. Dumas, A. Lu, S. Lefebvre, and C. WuDick, "By-example synthesis of structurally sound patterns," *ACM Transactions on Graphics*, vol. 34, no. 4, pp. 1–12, 2015.

[17] C. Torres, T. Campbell, N. Kumar, and E. Paulos, "Haptic Print: Designing Feel Aesthetics for Digital fabrication[C]," in *Proceedings of the 28th Annual ACM Symposium on User Interface Software & Technology*, pp. 583–591, ACM Press, New York, USA, November 2015.

[18] H. Takahashi and H. Miyashita, "Expressive fused deposition modeling by controlling extruder height and extrusion amount[C]," in *Proceedings of the CHI Conference on Human Factors in Computing Systems*, pp. 5065–5074, ACM Press, New York, USA, May 2017.

[19] R. Suzuki, T. Yeh, K. Yatani, and M. D. Gross, "Autocomplete Textures for 3D Printing," 2020.

[20] B. Gürsoy, "From control to uncertainty in 3D printing withclay[C]," in *Proceedings of the 36th International Conference on Education and Research in Computer Aided Architectural Design in Europe*, pp. 21–30, eCAADe Press, 2018.